J Arid Land (2023) 15(8): 887–900
https://doi.org/10.1007/s40333-023-0102-8

Science Press Springer-Verlag

Dividing the transit wind speeds into intervals as a favorable methodology for analyzing the relationship between wind speed and the aerodynamic impedance of vegetation in semiarid grasslands

LI Ruishen[1], PEI Haifeng[1], ZHANG Shengwei[1,2,3*], LI Fengming[4], LIN Xi[1], WANG Shuai[1], YANG Lin[1]

[1] College of Water Conservancy and Civil Engineering, Inner Mongolia Agricultural University, Hohhot 010018, China;
[2] Key Laboratory of Water Resources Protection and Utilization of Inner Mongolia Autonomous Region, Hohhot 010018, China;
[3] Autonomous Region Collaborative Innovation Center for Integrated Management of Water Resources and Water Environment in the Inner Mongolia Reaches of the Yellow River, Hohhot 010018, China;
[4] Inner Mongolia Autonomous Region Management Center of Sanshenggong Hydro-junction in the Yellow River, Bayannur 015200, China

Abstract: In grassland ecosystems, the aerodynamic roughness (Z_0) and frictional wind speed (u^*) contribute to the aerodynamic impedance of the grassland canopy. Thus, they are often used in the studies of wind erosion and evapotranspiration. However, the effect of wind speed and grazing measures on the aerodynamic impedance of the grassland canopy has received less analysis. In this study, we monitored wind speeds at multiple heights in grazed and grazing-prohibited grasslands for 1 month in 2021, determined the transit wind speed at 2.0 m height by comparing wind speed differences at the same height in both grasslands, and divided these transit wind speeds at intervals of 2.0 m/s to analyze the effect of the transit wind speed on the relationship among Z_0, u^*, and wind speed within the grassland canopy. The results showed that dividing the transit wind speeds into intervals has a positive effect on the logarithmic fit of the wind speed profile. After dividing the transit wind speeds into intervals, the wind speed at 0.1 m height ($V_{0.1}$) gradually decreased with the increase of Z_0, exhibiting three distinct stages: a sharp change zone, a steady change zone, and a flat zone; while the overall trend of u^* increased first and then decreased with the increase of $V_{0.1}$. Dividing the transit wind speeds into intervals improved the fitting relationship between Z_0 and $V_{0.1}$ and changed their fitting functions in grazed and grazing-prohibited grasslands. According to the computational fluid dynamic results, we found that the number of tall-stature plants has a more significant effect on windproof capacity than their height. The results of this study contribute to a better understanding of the relationship between wind speed and the aerodynamic impedance of vegetation in grassland environments.

Keywords: transit wind speeds; frictional wind speed; aerodynamic roughness; computational fluid dynamic (CFD); grazed grassland; grazing-prohibited grassland

Citation: LI Ruishen, PEI Haifeng, ZHANG Shengwei, LI Fengming, LIN Xi, WANG Shuai, YANG Lin. 2023. Dividing the transit wind speeds into intervals as a favorable methodology for analyzing the relationship between wind speed and the aerodynamic impedance of vegetation in semiarid grasslands. Journal of Arid Land, 15(8): 887–900. https://doi.org/10.1007/s40333-023-0102-8

*Corresponding author: ZHANG Shengwei (E-mail: zsw@imau.edu.cn)
Received 2022-10-08; revised 2023-02-14; accepted 2023-02-27

1 Introduction

The vegetation of typical grasslands in northern China is short, sparse, and vulnerable to degradation. Grazing disturbs the grassland canopy (Jäschke et al., 2020), which alters the surface aerodynamic impedance characteristics. The amount of standing grass residue is a key factor affecting the resistance of surface to wind erosion during non-growing season (Pi et al., 2020). The aerodynamic characteristics of the grassland canopy are crucial for studying the basic process of changes in soil physicochemical properties (Rauber et al., 2021) and soil–atmosphere gas exchange (Haghighi and Or, 2015). Therefore, research on the aerodynamic characteristics of the grassland canopy during non-growing season can guide climate models, wind meteorology, agro-pastoral production, and erosion hazard studies in pastoral areas (Levin et al., 2008).

The wind speed profile observations in grasslands can effectively describe the interrelationship between vegetation and air flow (Zhang et al., 2012). Different climatic characteristics (Yu et al., 2018), vegetation distributions, and leaf morphologies are key factors affecting the wind speed profile (Luo et al., 2020). The aerodynamic roughness (Z_0) of vegetation and frictional wind speed (u^*) are derived from the wind speed profile. These variables have been used to explain the relationship between vegetation and aerodynamic impedance in neutral atmospheric circumstances; Z_0 may be understood as the height from the ground with a wind speed of 0.0 m/s, while u^* is the shear effect of wind on the ground surface (Stull, 1988). For both Z_0 and u^*, extensive analyses have been conducted on field and indoor wind tunnel models. The wind resistance of the grassland canopy is mainly reflected in two aspects: branch deformation consumption and wind flow redistribution. Wind changes the morphology of vegetation (Liu et al., 2021). In grasslands, the taller the vegetation, the higher the degree of bending by the wind and the higher the rate of decline in windproof capacity. The flexibility and consequent bending of plants due to wind differ among species with similar aerodynamic characteristics (Kinugasa et al., 2021). The aerodynamic characteristics of the grassland canopy could be influenced by the quantity of very robust grass species. The mechanical strength of blade and the mass of blade per unit area determine the deformation of vegetation (Onoda et al., 2011). The low leaf density and plant height of overgrazed grassland considerably reduce wind resistance. The influence of grazing measures on plants alters the effect of wind on the grassland canopy. It is difficult to rebuild vegetation that has been eaten by animals in semiarid grasslands. We may utilize the consequences of long-term vegetation changes generated by grazing to better understand the link between grassland canopy and wind. Most studies have focused on wind rather than vegetation impedance (Fu et al., 2019; Liu et al., 2021; Xiong et al., 2021). The effect of increasing wind speed on Z_0 and u^* has been less studied. Modeling can determine the factors that affect the aerodynamic characteristics, because field observations may miss some details of variability.

Field monitoring of wind flow field is time-consuming and laborious. The computational fluid dynamics (CFD) is an effective research method and has been widely used. The CFD can simplify complex environmental conditions to analyze wind flow field, which is achieved through momentum and energy balance equations, such as the effect of artificial windproof measures on wind erosion and gravel transport (Xin et al., 2021). Numerical simulation method can replace the aerodynamic monitoring of tall trees (Zhang et al., 2022) with an accurate representation of wind and sand transport properties of shrubs at different locations (Gonzales et al., 2018). In this study area, the vegetation is short and sparse; therefore, it is difficult to determine the relationship between vegetation and wind speed. The CFD can bridge the gap in observation scale, while making it easier to quantify the relationship between wind speed and vegetation.

In this study, we monitored the vertical wind speed profiles in selected grazing-prohibited and grazed grasslands of the Eritu pasture in Inner Mongolia Autonomous Region of China. We used the variance test to determine the height of the transit wind speeds, and then divided the range of

the transit wind speeds into multiple intervals to study the aerodynamic characteristics of the grassland canopy. Additionally, the CFD was used for numerical simulation. The aims of this study were to select reasonable aerodynamic characteristic values for prolonged wind action and analyze the response of Z_0 and u^* within the grassland canopy to wind speed.

2 Methodology and data

2.1 Study area

The study area (42°05′–43°02′N, 114°05′–115°37′E; Fig. 1) is located in the Eritu pasture, Xilin Gol League, east-central Inner Mongolia Autonomous Region of China. The region has a mid-temperate semiarid continental climate with four distinct seasons, hot summer and cold winter, an annual average temperature of 1.9°C, and a maximum temperature of 34.9°C. The species in this study area mainly include *Artemisia frigida* Willd., *Stipa krylovii* Roshev., *Leymus chinensis* (Trin.) Tzvel., and *Cleistogenes squarrosa* (Trin.) Keng. South and southeast winds are predominant, with an annual average wind speed of 4.0 m/s.

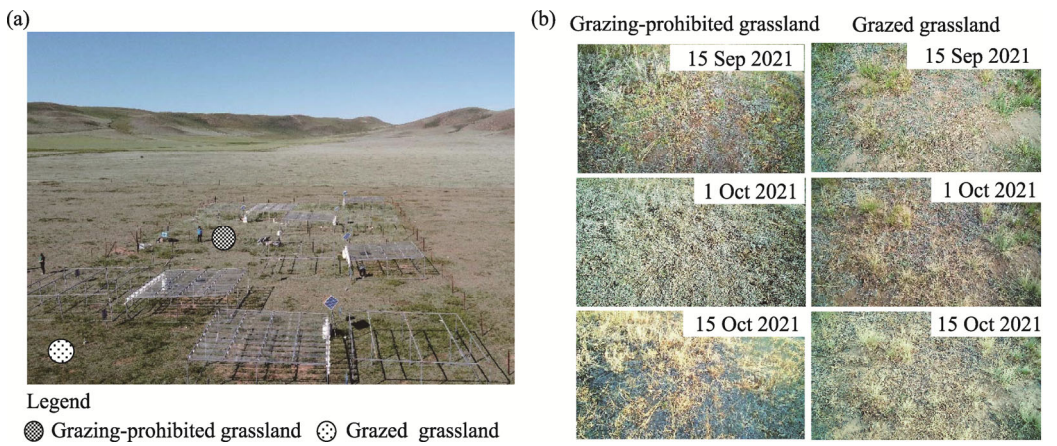

Fig. 1 Overview of the study area and experimental apparatus (a) and the images of vegetation growth in grazing-prohibited and grazed grasslands (b)

2.2 Experimental design

In order to observe the wind speed in grazing-prohibited and grazed grasslands, we conducted the experiment from 15 September to 15 October in 2021. We raised wether sheep (2 years old) on grazed grassland with a load rate of 2.45 sheep/hm^2, forming a heavily grazed grassland. In addition, a 30 m×30 m grazing-prohibited grassland was set up within grazed grassland. Grazing-prohibited grassland had been fenced for three years by the start of the investigation. The distance between grazed grassland and grazing-prohibited grassland was only 20 m, which makes it easier to compare their wind speed and vegetation.

2.3 Vegetation parameters of grassland

Vegetation is the basis of the experimental conditions in this study. Therefore, we conducted a vegetation survey in grazing-prohibited and grazed grasslands and selected three quadrats in each grassland (Fig. 2). The cover degree of a plant species in a quadrat was estimated using manual visual interpretation method, and the overall cover degree was computed using photographic data. The height of vegetation was measured with a ruler, and the total number of clumps was recorded. The height, cover degree, and number of each plant species were measured three times.

We conducted the vegetation survey in grazing-prohibited and grazed grasslands at the beginning and end of the experiment. Each vegetation survey was conducted using random sampling method, and rare species were excluded. Plant species with a height higher than 10 cm were classified as tall-stature plant (TSP), while those with a height less than 10 cm were sorted

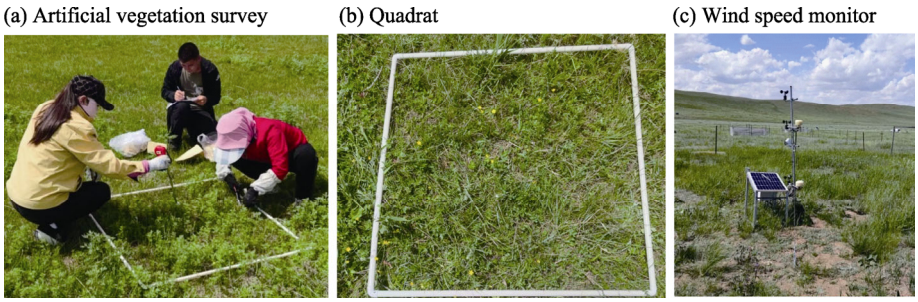

Fig. 2 Photos of artificial vegetation survey (a), quadrat (b), and wind speed monitor (c)

as short-stature plant (SSP). We only counted plant species with the cover degree exceeding 5.00% (Zheng et al., 2020). This experiment has a long observation period, so we used a digital camera to take photos of the vegetation conditions every 1 h to continuously record the vegetation growth status (Alberton et al., 2017). In this study, we showed the photos taken at three time points during the observation period (i.e., 15 September, 1 October, and 15 October in 2021; Fig. 1b), in which the cover degree of grazing-prohibited grassland was 37.55%, 38.09%, and 38.86%, respectively, and the cover degree of grazed grassland was 28.08%, 31.06%, and 30.62%, respectively. These values were calculated using the RGB (red, green, and blue) value method in Python (Alberton et al. 2017), which provides higher accuracy and continuity. The results calculated by RGB value method were slightly lower values than those obtained by manual visual interpretation method (Table 1). During the observation period, the photographic data showed slight changes in the cover degree of grazing-prohibited and grazed grasslands. The vegetation density of grazing-prohibited grassland was higher than that of grazed grassland, but the height of TSP in the two grasslands was similar.

Table 1 Vegetation characteristics of grazing-prohibited and grazed grasslands at the beginning and end of the experiment

Plant species	Functional group	The beginning of the experiment (15 September 2021)						The end of the experiment (15 October 2021)					
		Grazing-prohibited grassland			Grazed grassland			Grazing-prohibited grassland			Grazed grassland		
		NPS	CPS (%)	HPS (cm)	NPS	CPS (%)	HPS (cm)	NPS	CPS (%)	HPS (cm)	NPS	CPS (%)	HPS (cm)
Leymus chinensis (Trin.) Tzvel.	TSP	219 ±42	31.6 ±3.8	20.0 ±4.7	91 ±22	15.3 ±2.7	23.6 ±6.7	249 ±39	27.0 ±4.3	23.0 ±3.8	114 ±36	14.6 ±6.3	23.3 ±8.8
Cleistogenes squarrosa (Trin.) Keng	TSP	17±6	4.6±1.9	11.6±1.8	10±4	1.6±0.3	10.3±3.4	25±8	5.0±2.1	14.0±4.7	11±4	0.6±0.8	10.3±3.3
Stipa krylovii Roshev.	TSP	49±18	4.5±1.2	10.2±0.9	21±6	5.3±1.5	12.2±5.3	79±20	17.6±4.5	12.0±3.6	57±19	7.0±2.6	11.0±2.9
Artemisia frigida Willd.	SSP	-	10.0±3.4	4.2±0.9	-	13.3±2.8	4.2±1.1	-	8.6±2.1	5.0±0.7	-	4.3±1.4	8.3±2.9
Total	-	285	30.8	-	122	28.1	-	353	38.9	-	182	30.6	-

Note: TSP, tall-stature plant, representing the plant species with a height higher than 10 cm; SSP, short-stature plant, representing the plant species with a height less than 10 cm; NPS, the number of plant species; CPS, the cover degree of plant species; HPS, the height of plant species; -, no data. For *Artemisia frigida* Willd., we replaced NPS with CPS because the species is tiny and dense. Mean±SD.

2.4 Numerical simulation

The CFD between wind speed and vegetation was performed using Ansys Fluent 2022 software. We developed a geometric model using the measured vegetation data. Table 1 shows the vegetation data of grazing-prohibited and grazed grasslands. We built the model using the height

and cover degree, while ignoring the number of plant species. The weight of average height of vegetation model (ΔH; cm) was calculated as follows:

$$\Delta\mathrm{CPS} = \mathrm{CPS}(L.\ chinensis) + \mathrm{CPS}(C.\ squarros) + \mathrm{CPS}(S.\ krylovii), \quad (1)$$

$$\Delta\mathrm{H} = \frac{[\mathrm{HPS}(L.\ chinensis)\times\mathrm{CPS}(L.\ chinensis) + \mathrm{HPS}(C.\ squarrosa)\times \mathrm{CPS}(C.\ squarrosa) + \mathrm{HPS}(S.\ krylovii)\times\mathrm{CPS}(S.\ krylovii)]}{\Delta\mathrm{CPS}}, \quad (2)$$

where ΔCPS (%) is the total cover degree of *L. chinensis*, *C. squarrosa*, and *S. krylovii*, including the cover degree of the overlapping parts of each plant species; CPS (%) is the cover degree of plant species; and HPS (cm) is the height of plant species. The vegetation in the experimental region is largely made up of elongated leaves, and the model used in this study notes this trait. The turbulence model in the CFD is *k*-epsilon, which can be used under most conditions. The wall conditions of the CFD referred to Z_0 measured in the field. Finally, we used the Gauss-Seidel iterative method for 500 iterations until the results converged to the specified accuracy.

2.5 Transit wind speeds and wind speed characteristic value

Wind speeds at heights of 0.1, 0.4, 0.6, 1.2, and 2.0 m above the ground were observed using wind cups (RS-FSJT, Renko Measurement and Control Technology Company, Shandong Province, China) in both grazing-prohibited grassland and grazed grassland. The measurement accuracy and interval of the wind cups are 0.1 m/s and 20 min, respectively. All data were collected through a data collector (CR1000X, Cambell, Utah, America). Wind speed usually shows an increasing trend with the increase of distance from the ground (Stanhill, 1969; de Souza et al., 2016). We found that there was no significant difference in the wind speed at 2.0 m height ($V_{2.0}$) between grazing-prohibited grassland and grazed grassland based on the analysis of variance. Therefore, the $V_{2.0}$ was used as the transit wind speed. In this study, the plant height ranges from 10 to 20 cm, so the wind speed at 0.1 m height ($V_{0.1}$) was used as the wind speed within the grassland canopy. In order to more easily analyze $V_{0.1}$ and the aerodynamic characteristics of grassland, we selected the wind speed of 2.0 m/s as interval and classified the transit wind speeds into five categories, including 0.0–2.0, 2.0–4.0, 4.0–6.0, 6.0–8.0, and 8.0–10.0 m/s. The logarithmic fitting function of height and wind speed can be obtained from the wind speed profile (Stanhill, 1969). In order to make the wind speed profile representative and prevent meteorological factors such as temperature and humidity from affecting airflow stability (Du et al., 2017), we selected the wind speed profile with the coefficient of determination (R^2)>0.75 in this study. The wind speed profile is often modelled using the log profile equation, and the equation is as follows:

$$Uz = A + B\ln z, \quad (3)$$

where z is the height above the ground (m); Uz is the wind speed at the height of z (m/s); and A and B are the regression coefficients.

The u^* (m/s) represents the shear stress caused by wind action and is calculated as follows (Dong et al., 2001):

$$u^* = UzK/\ln\left(\frac{z-d}{Z_0}\right), \quad (4)$$

where Z_0 is aerodynamic roughness (mm); K is the von-Kammen constant, usually taken as 0.4; and d is the zero-plane displacement (mm), indicating the height of momentum absorbed by a single rough element, which can be calculated using the following equation (Li et al., 2015):

$$\log_{10} d = 0.979\log_{10}\mathrm{HPS} - 0.154. \quad (5)$$

2.6 Screening method based on wind speed data of the aerodynamic roughness (Z_0)

In this study, we measured the wind speed profiles of grazing-prohibited and grazed grasslands and determined $V_{2.0}$. The processing flow of these data is shown in Figure 3, which facilitates the analysis of the relationship between Z_0 and u^*.

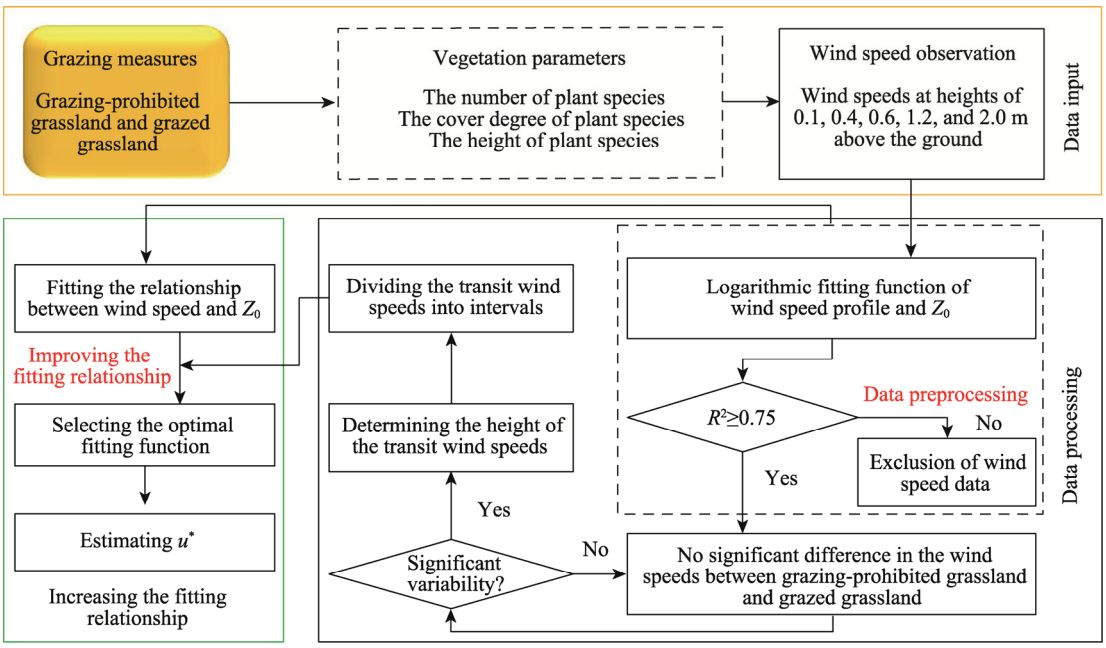

Fig. 3 Flowchart used in this study for enhancing the relationship between the aerodynamic roughness (Z_0) and frictional wind speed (u^*)

3 Results

3.1 Effect of the transit wind speeds on the wind speed at 0.1 m height ($V_{0.1}$)

It can be seen from Figure 4 that $V_{0.1}$ was related to the frequency of the transit wind speed. For different grazing measures (i.e., grazing-prohibited grassland and grazed grassland), when the transit wind speeds were less than 5.0 m/s, the frequency of transit wind speed differed significantly. The $V_{0.1}$ of 0.0–2.0 and 5.0–8.0 m/s in both grazing-prohibited grassland and grazed grassland was made up of the same transit wind speed, which mainly caused the difference in $V_{0.1}$ in the range of 2.0–5.0 m/s. For example, the $V_{0.1}$ of 2.0–4.0 m/s in grazing-prohibited grassland was influenced by the transit wind speed of 8.0–10.0 m/s. This result indicated that grazing-prohibited grassland has a stronger ability to restrain the strong transit wind speeds.

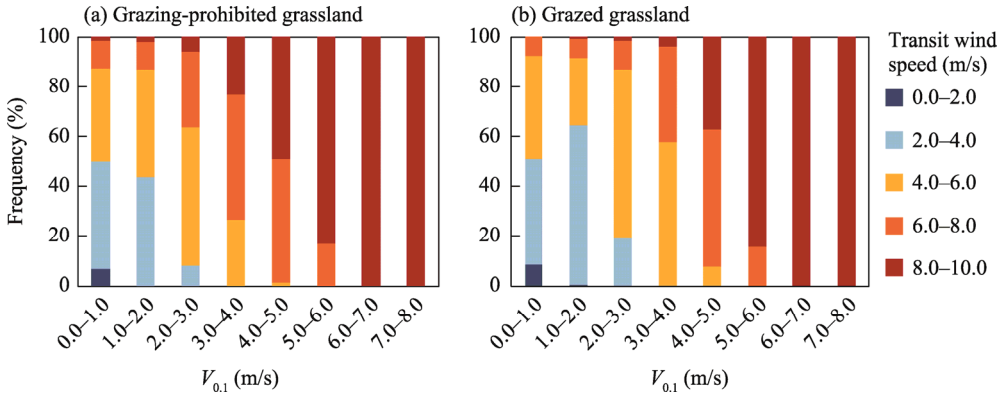

Fig. 4 Frequency of different transit wind speeds at the wind speed at 0.1 m height ($V_{0.1}$) in grazing-prohibited grassland (a) and grazed grassland (b)

Table 2 shows that there was no significant difference in $V_{2.0}$ between grazing-prohibited grassland and grazed grassland. Due to the low canopy of grassland, the effect of vegetation on

wind speed gradually decreased with the increase of the height above the ground. In addition to 0.0–2.0 m/s transit wind speed, there were significant differences in $V_{0.1}$ between grazing-prohibited grassland and grazed grassland at the transit wind speeds of 2.0–4.0, 4.0–6.0, 6.0–8.0, and 8.0–10.0 m/s. The R^2 of logarithmic function of the wind speed profile was relatively large (R^2>0.85), but the R^2 showed a decreasing trend with the increase of the transit wind speed in grazed grassland. The characteristics of grasslands and the speed of the transit wind speeds caused the change in logarithmic fitting, and the transit wind speeds influenced the calculation of Z_0. The fitting relationship between Z_0 and $V_{0.1}$ showed a decreasing trend in grazing-prohibited grassland, while it increased first and then decreased in grazed grassland.

Table 2 Parameters related to the wind speed profile in grazing-prohibited and grazed grasslands

Grazing measure	Transit wind speed (m/s)	Wind speed at 2.0 m height ($V_{2.0}$; m/s)	Wind speed at 0.1 m height ($V_{0.1}$; m/s)	*A*	*B*	R^2
Grazing-prohibited grassland	0.0–2.0	1.4±0.6	0.4±0.3	–0.12	0.26	0.89
	2.0–4.0	3.2±0.5	1.2±0.7*	0.62	–0.07	0.96
	4.0–6.0	5.0±0.5	1.9±1.1*	0.96	–0.04	0.98
	6.0–8.0	6.8±0.5	3.0±1.2*	0.29	1.24	0.99
	8.0–10.0	8.2±0.5	3.9±1.0*	0.21	1.58	0.98
Grazed grassland	0.0–2.0	1.4±0.5	0.4±0.3	–0.41	0.31	0.99
	2.0–4.0	3.1±0.5	1.3±0.7*	–0.02	0.61	0.99
	4.0–6.0	5.0±0.5	2.4±1.1*	0.49	0.84	0.99
	6.0–8.0	6.8±0.5	3.8±1.2*	1.46	0.96	0.96
	8.0–10.0	8.8±0.5	5.3±0.9*	2.24	3.37	0.87

Note: *A* and *B* are the regression coefficients calculated by Equation 3. "*" represents the significance difference in wind speed between grazing-prohibited grassland and grazed grassland for the same transit wind speed (P<0.05).

3.2 Effect of wind speed on Z_0

As shown in Figure 5, Z_0 of both grazing-prohibited grassland and grazed grassland tended to decrease with the increase of the transit wind speeds. The Z_0 of grazing-prohibited grassland decreased rapidly at lower transit wind speeds; while the Z_0 of grazed grassland decreased rapidly at higher transit wind speeds. The Z_0 of grazing-prohibited grassland was higher than that of grazed grassland when the transit wind speed was the same.

The Z_0 was mainly concentrated in higher transit wind speeds and tended to decrease with the increase of the transit wind speeds (Fig. 5 b–f). The $V_{0.1}$ tended to decrease with the increase of Z_0 (Fig. 5f). It can be seen from Figure 5 that there were three stages in each interval of the transit wind speeds from 2.0 to 8.0 m/s, including a sharp change zone, a steady change zone, and a flat zone. The sharp change zone disappeared at the 8.0–10.0 m/s transit wind speed (Fig. 5f), indicating that the variation in Z_0 was relatively smooth at higher transit wind speeds.

We simulated the expressions of Z_0 as a function of $V_{0.1}$ in grazing-prohibited and grazed grasslands, as shown in Table 3. By comparing the R^2, we can see that dividing the transit wind speeds into intervals improved the fitting relationship between $V_{0.1}$ and Z_0. A slight decrease in the R^2 occurred in grazing-prohibited grassland at the 0.0–2.0 m/s transit wind speed and in grazed grassland at 8.0–10.0 m/s transit wind speed, which may be caused by the change in canopy structure, indicating that dividing the transit wind speeds into intervals may affect the relationship between $V_{0.1}$ and Z_0.

3.3 Effect of wind speed on frictional wind speed (u^*)

In grazing-prohibited and grazed grasslands, the u^* increased with the increase of the transit wind speeds (Fig. 6). The u^* of grazing-prohibited grassland was significantly higher than that of grazed grassland, indicating that grazing-prohibited grassland had better wind resistance with the increase of wind speed.

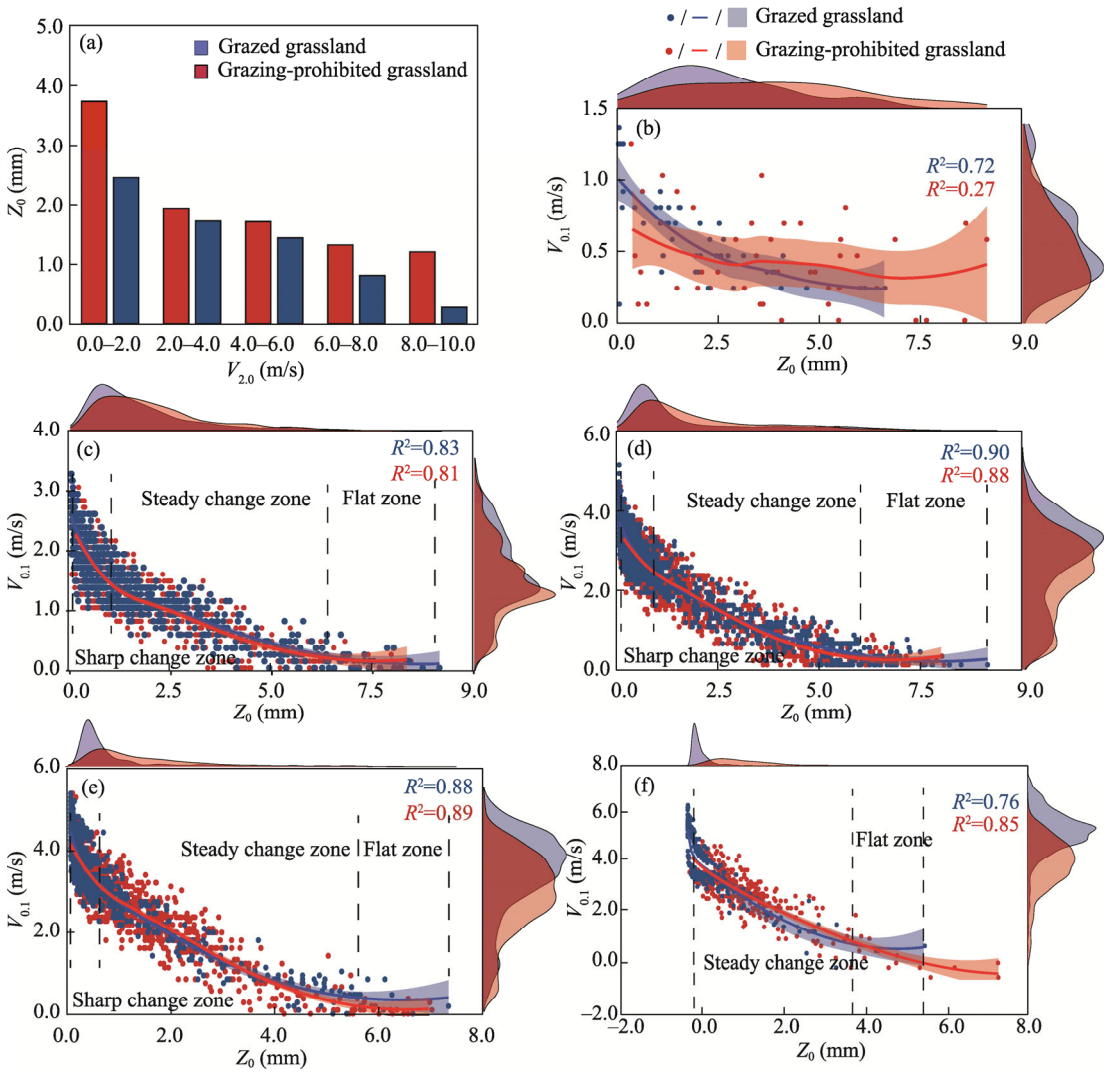

Fig. 5 (a), relationship between the wind speed at 2.0 m height ($V_{2.0}$) and Z_0; (b–f), relationship between Z_0 and $V_{0.1}$ at the transit wind speeds of 0.0–2.0, 2.0–4.0, 4.0–6.0, 6.0–8.0, and 8.0–10.0 m/s, respectively. For figure b–f, the shaded areas on the right side of *y*-axis and the upper side of *x*-axis are the probability densities of $V_{0.1}$ and Z_0, respectively, and the shaded areas inside each figure represent 95% confidence interval.

Table 3 Z_0 as a function of $V_{0.1}$ for different transit wind speeds

Transit wind speed (m/s)	Grazing-prohibited grassland		Grazed grassland	
	Function expression	R^2	Function expression	R^2
0.0–2.0	$V_{0.1}=0.852e^{-0.21Z_0}$	0.58	$V_{0.1}=-0.16\ln(Z_0)+0.655$	0.78
2.0–4.0	$V_{0.1}=1.970e^{-0.34Z_0}$	0.73	$V_{0.1}=2.057e^{-0.33Z_0}$	0.82
4.0–6.0	$V_{0.1}=3.315e^{-0.43Z_0}$	0.81	$V_{0.1}=3.310e^{-0.40Z_0}$	0.87
6.0–8.0	$V_{0.1}=4.683e^{-0.44Z_0}$	0.82	$V_{0.1}=4.474e^{-0.38Z_0}$	0.87
8.0–10.0	$V_{0.1}=5.609e^{-0.35Z_0}$	0.76	$V_{0.1}=5.643e^{-0.36Z_0}$	0.74
General	$V_{0.1}=3.686e^{-0.42Z_0}$	0.64	$V_{0.1}=3.683e^{-0.43Z_0}$	0.76

There was no significant regular variation between u^* and $V_{0.1}$ at the 0.0–2.0 m/s transit wind speed (Fig. 6b). At the transit wind speeds of 2.0–4.0, 4.0–6.0, 6.0–8.0, and 8.0–10.0 m/s, the

relationship between u^* and $V_{0.1}$ showed an increasing trend followed by a decreasing trend (Fig. 6c–f). The clustering degree of $V_{0.1}$ and u^* decreased with the increase of the transit wind speed, and this effect was more pronounced in grazed grassland.

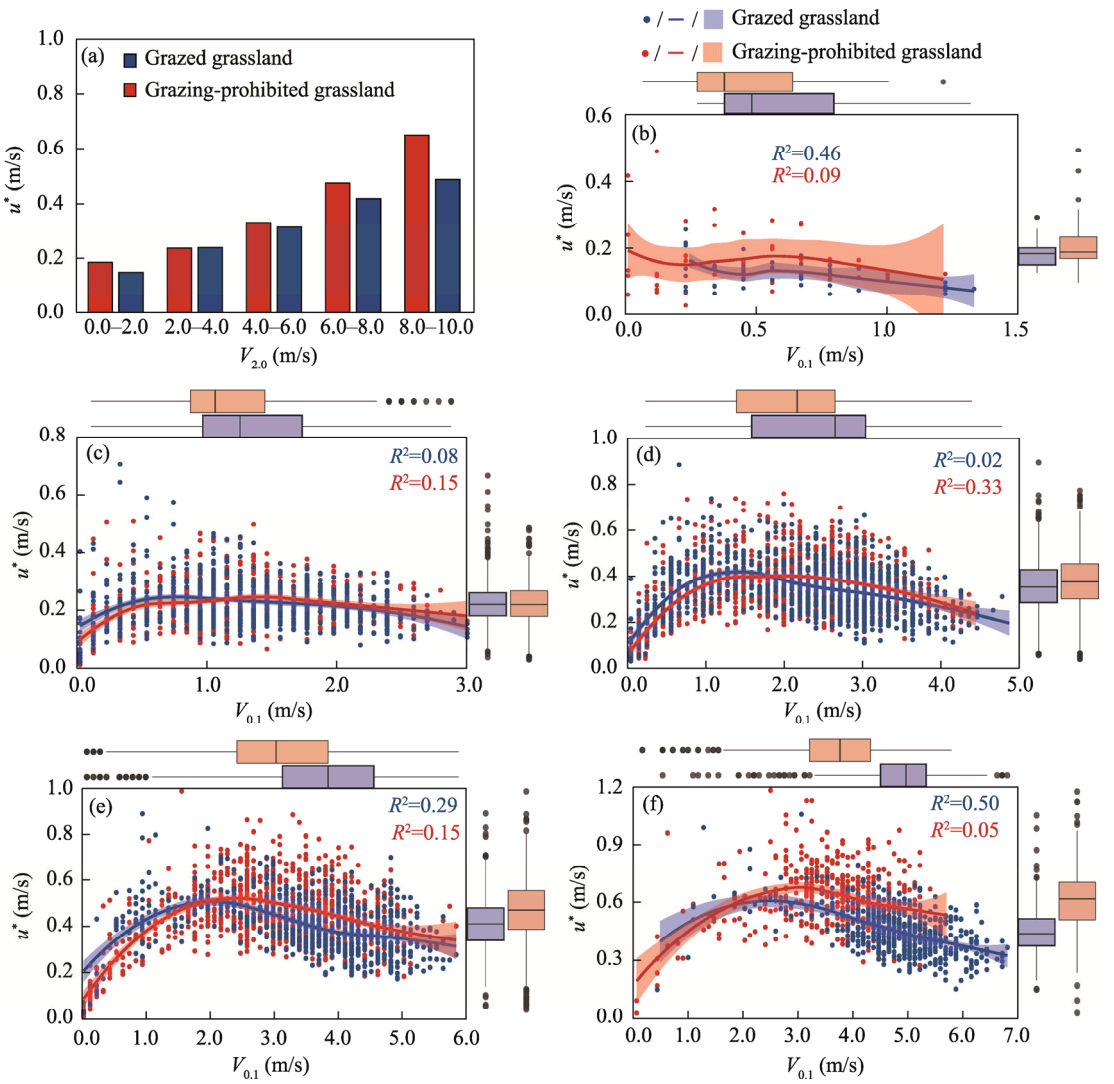

Fig. 6 (a), relationship between $V_{2.0}$ and frictional wind speed (u^*); (b–f), relationship between $V_{0.1}$ and u^* at the transit wind speeds of 0.0–2.0, 2.0–4.0, 4.0–6.0, 6.0–8.0, and 8.0–10.0 m/s, respectively. For figure b–f, in the box plot, the upper and lower limits of the box indicate the 75th and 25th percentile values, respectively; the horizontal lines in each box represent the median; the upper and lower whiskers show the maximum and minimum values, respectively; and the scattered points are outliers. The shaded areas inside each figure represent 95% confidence interval.

3.4 Effect of the transit wind speeds on the relationship between u^* and Z_0

In order to explain the effect of the transit wind speeds on the relationship between u^* and Z_0, we used the ratio of the transit wind speeds to u^* (u/u^*). As shown in Figure 7, Z_0 showed a logarithmic decrease with the increase of u/u^*. When u/u^* was greater than 20, there were many discrete points, with Z_0 greater than 1.76 and 0.98 mm in grazing-prohibited and grazed grasslands, respectively.

We fitted the relationship between Z_0 and the average values of u^* after dividing the transit wind speeds into intervals and found that Z_0 decreased with the increase of u^* (Fig. 7b). In addition, in grazing-prohibited grassland, there was a power function relationship between Z_0 and

the average values of u^* after dividing the transit wind speeds into intervals; while, in grazed grassland, the relationship was liner.

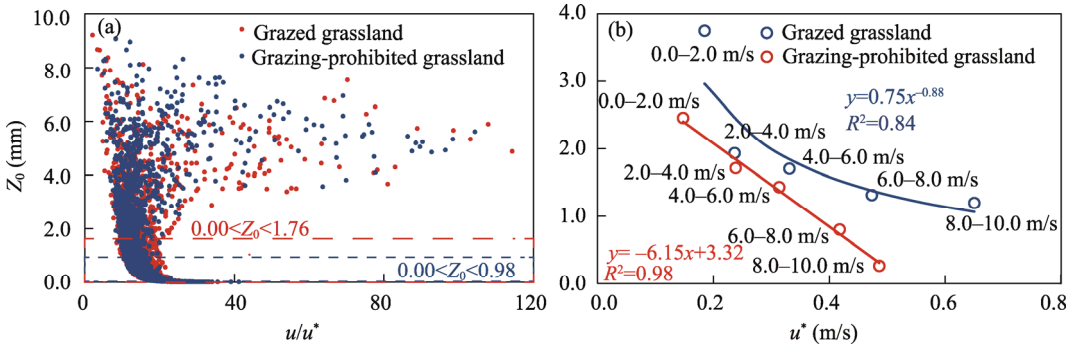

Fig. 7 (a), relationship between the ratio of the transit wind speeds to u^* (u/u^*) and Z_0; (b), relationship between Z_0 and the average values of u^* after dividing the transit wind speeds into intervals (0.0–2.0, 2.0–4.0, 4.0–6.0, 6.0–8.0, and 8.0–10.0 m/s)

3.5 Computational fluid dynamic (CFD) simulation of wind flow field

The CFD model was used to simulate the difference of wind flow field between grazing-prohibited grassland and grazed grassland. The transit wind speeds of 2.0, 5.0, and 10.0 m/s were used as examples (Fig. 8). In grazing-prohibited and grazed grasslands, the 2.0 m/s transit wind speed had similar effects on $V_{0.1}$ (Fig. 8a and b). The 5.0 m/s transit wind speed significantly increased $V_{0.1}$ in grazed grassland. The 10.0 m/s transit wind speed had a greater effect on the overall wind flow field in grazing-prohibited grassland than in grazed grassland. This phenomenon indicated that the density of vegetation was a key factor affecting the wind speed profile. Near the grassland canopy, the density of vegetation can direct more wind away

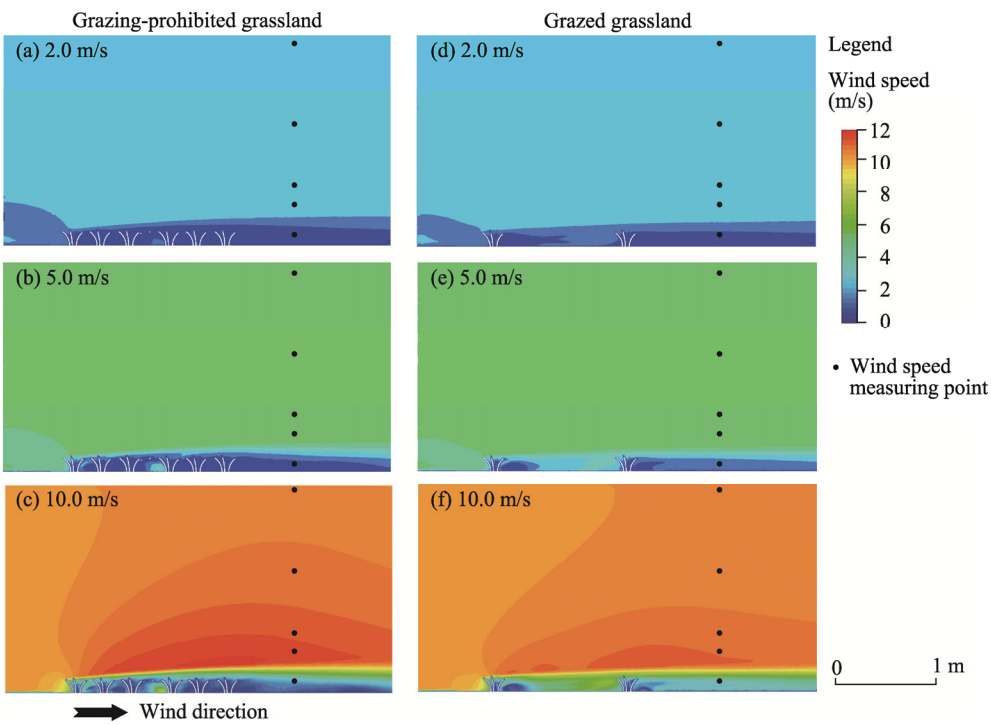

Fig. 8 Front view of computational fluid dynamic (CFD) simulation at the transit wind speeds of 2.0, 5.0, and 10.0 m/s in grazing-prohibited grassland (a–c) and grazed grassland (d–f)

from the ground. With the increase of height, the difference of wind flow field between grazing-prohibited grassland and grazed grassland decreased. These results showed that $V_{2.0}$ was minimally influenced by the differences in surface vegetation. Therefore, dividing the transit wind speeds into intervals can better analyze the effect of vegetation differences on the wind speed profile.

In addition, we also calculated the wind flow field in grazing-prohibited and grazed grasslands using the CFD simulation (Fig. 9). The result showed that the wind deflecting effect of vegetation was the main way to reduce $V_{0.1}$, which was more evident in grazing-prohibited grassland. With the increase of wind speed, the windproof effect of grazing-prohibited grassland became more obvious.

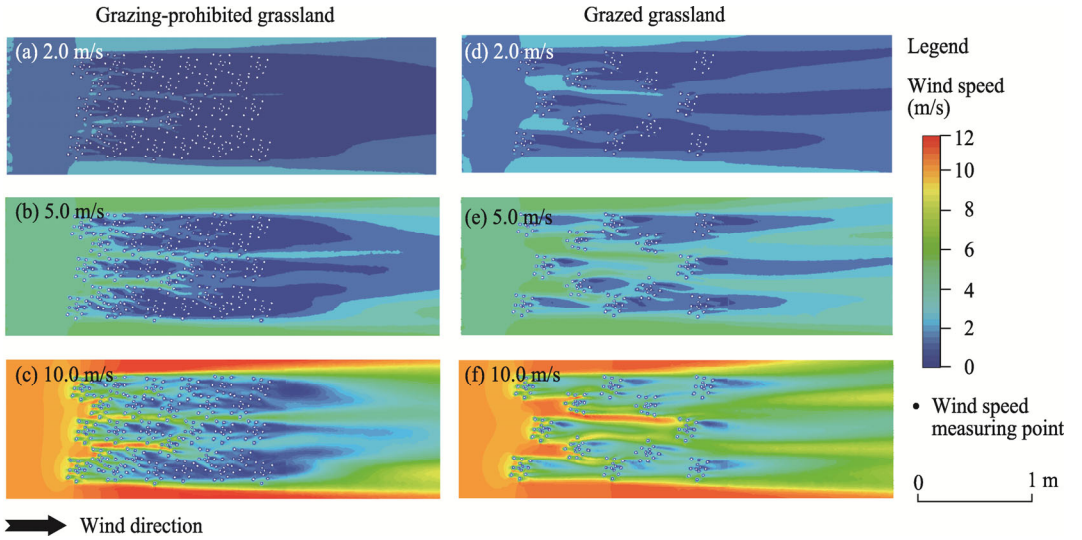

Fig. 9 Top view (at 0.1 m height) of CFD simulation at the transit wind speeds of 2.0, 5.0, and 10.0 m/s in grazing-prohibited grassland (a–c) and grazed grassland (d–f). The white points are the position of the geometric model in the wind flow field.

4 Discussion

4.1 Aerodynamic effects of grazing measures

The height and density of grassland vegetation are key factors affecting aerodynamics (Kang et al., 2019). Grazing is the main ecological utilization of arid and semiarid grasslands. The trampling and chewing by livestock caused changes in the characteristics of vegetation (Jäschke et al., 2020). Heavily grazed grassland will cause community degradation, as evidenced by the large growth of short-stature plants (Török et al., 2018). Thus, the effect of different grazing measures on the grassland canopy changes the aerodynamic impedance of vegetation. In this study, the number of tall-stature plants was significantly higher in grazing-prohibited grassland than that in grazed grassland (Table 1). There were differences in the effects of vegetation characteristics on the transit wind speed. For example, when the transit wind speed was higher (8.0–10.0 m/s), the maximum value of Z_0 was approximately 5.7 mm in grazed grassland and 7.5 mm in grazing-prohibited grassland. Grazing-prohibited grassland had a higher blocking effect on $V_{0.1}$ (Fig. 5f). This phenomenon is mainly due to the deformation of the top of the grassland canopy caused by the wind action. The dense vegetation in grazing-prohibited grassland is more resistant to this deformation (Kinugasa et al., 2021). According to the CFD results (Fig. 8), we found that the number of tall-stature plants has a more significant effect on windproof capacity than their height. For sparse grasslands, individuals of tall-stature plants are particularly important for optimal wind blocking of the canopy, but the process of reducing wind speed in fine-leaved vegetation is more dependent on the number of plants than their height, which is influenced by

leaf morphology (Miri et al. 2017). This conclusion is the same as in this study, and we found that grazing does not affect the height of tall-stature plants by counting the number of plants in a wide range of species, which may be related to the selective herbivorous behavior of livestock (Zanella et al. 2021). In summary, grazing-prohibited grassland reduce surface aerodynamics mainly due to higher densities of tall-stature plants.

The leaves of grasses in arid areas are slender and the plants are mostly clumped. Each clump of plant can be seen as a roughness element with discrete distribution. In some wind tunnel experiments, physical models, such as cylinders, cones, and inverted truncated cones, have been used to simulate roughness element (Liu et al., 2021). Undeniably, such research methods reduce the experimental workload and reach similar conclusions as field tests. However, the dissimilarities between plant leaves are neglected, which is one of the main differences caused by grazing measures (Yan et al., 2015). The CFD simulation avoids this problem very well.

4.2 Influencing factors of Z_0 and u^*

The wind speed profile is a common monitoring method for the surface wind flow field. The logarithmic function provides sufficient fitting conditions to derive Z_0 and u^*. However, the time interval and height of the wind speed monitoring can affect the accuracy of Z_0 and u^* calculations using the wind speed profile (Bañuelos-Ruedas et al., 2010). Differences between daily data and hourly data can also result in different Z_0 and u^* (Yu et al., 2018). The fluctuation of wind speed on different time scales affects the expression of aerodynamic characteristics (Liu et al., 2022). The difference in Z_0 and u^* generated by the time scale seems to be related to the changes in aerodynamic resistance of plant leaves caused by wind deformation (Walter et al., 2012). The results of this study showed that aerodynamic characteristics are influenced by the selection of wind data and vegetation. Therefore, deriving Z_0 and u^* using the fitted functions of the wind speed profile still requires knowing whether it is affected by changes in the wind speed flow field caused by vegetation, which will affect the functional expressions (Barnéoud and Ek, 2019). The CFD results indicated that compared to grazed grassland, there was a greater difference in wind flow field of grazing-prohibited grassland as the height increases. In addition, deriving a more optimal functional relationship between Z_0 and u^* can avoid parameter calculation errors caused by sudden changes in the instantaneous wind speed profile.

5 Conclusions

In this study, we divided the transit wind speeds into five intervals, studied the effects of different transit wind speeds and vegetation parameters on wind speed within the grassland canopy, and analyzed the relationship of Z_0 and u^* to $V_{0.1}$ in grazing-prohibited and grazed grasslands of Eritu pasture. The relationship between wind speed and vegetation was explored by using the CFD simulation. The results showed that, with the increase of the transit wind speeds, the fitting relationship between Z_0 and $V_{0.1}$ showed a decreasing trend in grazing-prohibited grassland, while it increased first and then decreased in grazed grassland. With the increase of Z_0, $V_{0.1}$ roughly showed three stages: a sharp change zone, a steady change zone, and a flat zone; and the sharp change zone disappeared at the 8.0–10.0 m/s transit wind speed in grazing-prohibited grassland. The fitting relationship between Z_0 and $V_{0.1}$ was improved by dividing the transit wind speeds into intervals. In semiarid grasslands with spare vegetation, the number of tall-stature plants had a more significant effect on windproof capacity than their height. By dividing the transit wind speeds into intervals, this study advances our knowledge of the link between wind speed and grassland canopy, and offers a theoretical framework for further clarifying the mechanism of aerodynamic effect on grassland.

Conflict of interest

The authors declare that they have no known competing financial interests or personal relationships that could have appeared to influence the work reported in this paper.

Acknowledgements

This research was funded by the National Natural Science Foundation of China (52279017 and 52079063), Technological Achievements of Inner Mongolia Autonomous Region of China (2020CG0054 and 2022YFDZ0050), the Graduate Education Innovation Program of Inner Mongolia Autonomous Region of China (B20210188Z), and the Program for Innovative Research Team in Universities of Inner Mongolia Autonomous Region, China (NMGIRT2313). The authors would like to thank the editors and anonymous reviewers for their constructive comments, which contributed to the improvement of this manuscript.

Author contributions

Conceptualization: LI Ruishen, ZHAGN Shengwei; Data curation: LIN Xi; Methodology: LI Ruishen; Investigation: WANG Shuai; Formal analysis: LIN Xi; Writing original draft preparation: LI Ruishen; Writing review and editing: LI Ruishen; Funding acquisition: ZHANG Shengwei; Resources: LI Fengming; Supervision: ZHANG Shengwei; Project administration: YANG Lin; Software: YANG Lin; Validation: LI Fengming; Visualization: WANG Shuai.

References

Alberton B, Torres R d S, Cancian L F, et al. 2017. Introducing digital cameras to monitor plant phenology in the tropics: applications for conservation. Perspectives in Ecology and Conservation, 15(2): 82–90.

Bañuelos-Ruedas F, Angeles-Camacho C, Rios-Marcuello S. 2010. Analysis and validation of the methodology used in the extrapolation of wind speed data at different heights. Renewable and Sustainable Energy Reviews, 14(8): 2383–2391.

Barnéoud P, Ek N. 2019. On the Application of linear regression to surface-layer wind profiles for deducing roughness length and friction velocity. Boundary-Layer Meteorology, 174(2): 327–339.

de Souza C M, Dias-Júnior C Q, Tóta J, et al. 2016. An empirical-analytical model of the vertical wind speed profile above and within an Amazon forest site. Meteorological Applications, 23(1): 158–164.

Dong Z B, Gao S Y, Fryreart D W. 2001. Drag coefficients, roughness length and zero-plane displacement height as disturbed by artificial standing vegetation. Journal of Arid Environments, 49(3): 485–505.

Du H Q, Wang T, Xue X. 2017. Field determination for roughness length above the different non-erodible surfaces. Sciences in Cold and Arid Regions, 9(1): 67–77.

Fu L T, Fan Q, Huang Z L. 2019. Wind speed acceleration around a single low solid roughness in atmospheric boundary layer. Scientific Reports, 9(1): 12002, doi: 10.1038/s41598-019-48574-7.

Gonzales H B, Ravi S, Li J R, et al. 2018. Ecohydrological implications of aeolian sediment trapping by sparse vegetation in drylands. Ecohydrology, 11(7): e1986, doi: 10.1002/eco.1986.

Haghighi E, Or D. 2015. Interactions of bluff-body obstacles with turbulent airflows affecting evaporative fluxes from porous surfaces. Journal of Hydrology, 530: 103–116.

Jäschke Y, Heberling G, Wesche K. 2020. Environmental controls override grazing effects on plant functional traits in Tibetan rangelands. Functional Ecology, 34(3): 747–760.

Kang L Q, Zhang J J, Zou X Y, et al. 2019. Experimental investigation of the aerodynamic roughness length for flexible plants. Boundary-Layer Meteorology, 172(3): 397–416.

Kinugasa T, Sagayama T, Gantsetseg B, et al. 2021. Effect of simulated grazing on sediment trapping by single plants: A wind-tunnel experiment with two grassland species in Mongolia. CATENA, 202: 105262, doi: 10.1016/j.catena.2021.105262.

Levin N, Ben-Dor E, Kidron G J, et al. 2008. Estimation of surface roughness (z_0) over a stabilizing coastal dune field based on vegetation and topography. Earth Surface Processes and Landforms, 33(10): 1520–1541.

Li X, Feng G, Sharratt B, et al. 2015. Aerodynamic properties of agricultural and natural surfaces in northwestern Tarim Basin. Agricultural and Forest Meteorology, 204: 37–45.

Liu J Q, Kimura R, Miyawaki M, et al. 2021. Effects of plants with different shapes and coverage on the blown-sand flux and roughness length examined by wind tunnel experiments. CATENA, 197: 104976, doi: 10.1016/j.catena.2020.104976.

Liu X Y, Zhang C L, Zhang H, et al. 2022. Characteristics of wind velocity pulsation and its relation to average wind velocity and friction wind velocity. Bulletin of Soil and Water Conservation, 40(5): 60–63, 78. (in Chinese)

Luo Q, Zhen L, Xiao Y, et al. 2020. The effects of different types of vegetation restoration on wind erosion prevention: A case study in Yanchi. Environmental Research Letters, 15(11): 115001, doi: 10.1088/1748-9326/abbaff.

Miri A, Dragovich D, Dong Z B. 2017. Vegetation morphologic and aerodynamic characteristics reduce aeolian erosion. Scientific Reports, 7: 12831, doi: 10.1038/s41598-017-13084-x.

Onoda Y, Westoby M, Adler P B, et al. 2011. Global patterns of leaf mechanical properties. Ecology Letters, 14(3): 301–312.

Pi H, Huggins D R, Sharratt B. 2020. Threshold friction velocities influenced by standing crop residue in the inland Pacific Northwest, USA. Land Degradation and Development, 31(16): 2356–2368.

Rauber L R, Sequinatto L, Kaiser D R, et al. 2021. Soil physical properties in a natural highland grassland in southern Brazil subjected to a range of grazing heights. Agriculture, Ecosystems and Environment, 319: 107515, doi: 10.1016/j.agee.2021.107515.

Stanhill G. 1969. A simple instrument for the field measurement of turbulent diffusion flux. Journal of Applied Meteorology and Climatology, 8(4): 509–513.

Stull R B. 1988. An Introduction to Boundary Layer Meteorology. New York: Springer Science and Business Media.

Török P, Penksza K, Tóth E, et al. 2018. Vegetation type and grazing intensity jointly shape grazing effects on grassland biodiversity. Ecology and Evolution, 8(20): 10326–10335.

Walter B, Gromke C, Leonard K C, et al. 2012. Spatio-temporal surface shear-stress variability in live plant canopies and cube arrays. Boundary-Layer Meteorology, 143(2): 337–356.

Xin G W, Huang N, Zhang J, et al. 2021. Investigations into the design of sand control fence for Gobi buildings. Aeolian Research, 49: 100662, doi: 10.1016/j.aeolia.2020.100662.

Xiong P F, Chen Z F, Zhou J J, et al. 2021. Aboveground biomass production and dominant species type determined canopy storage capacity of abandoned grassland communities on semiarid Loess Plateau. Ecohydrology, 14(2): e2265, doi: 10.1002/eco.2265.

Yan R R, Xin X P, Yan Y C, et al. 2015. Impacts of differing grazing rates on canopy structure and species composition in Hulunber meadow steppe. Rangeland Ecology and Management, 68(1): 54–64.

Yu M Z, Wu B F, Zeng H W, et al. 2018. The impacts of vegetation and meteorological factors on aerodynamic roughness length at different time scales. Atmosphere, 9(4): 149, doi: 10.3390/atmos9040149.

Zanella P G, Junior L H P D G, Pinto C E, et al. 2021. Grazing intensity drives plant diversity but does not affect forage production in a natural grassland dominated by the tussock-forming grass *Andropogon lateralis* Nees. Scientific Reports, 11(1): 16744, doi: 10.1038/s41598-021-96208-8.

Zhang Q, Zeng J, Yao T. 2012. Interaction of aerodynamic roughness length and windflow conditions and its parameterization over vegetation surface. Chinese Science Bulletin, 57(13): 1559–1567.

Zhang W, Wu J J, Jiang A. 2022. Numerical study on aerodynamic roughness of forest. Earth Science Informatics, 15(1): 465–472.

Zheng M M, Song J, Ru J Y, et al. 2020. Effects of grazing, wind erosion, and dust deposition on plant community composition and structure in a temperate steppe. Ecosystems, 24(2): 403–420.